Journal of Materials Chemistry A

Accepted Manuscript

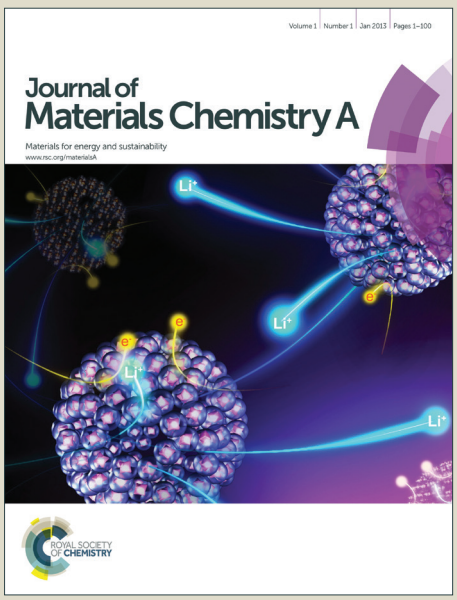

This is an *Accepted Manuscript*, which has been through the Royal Society of Chemistry peer review process and has been accepted for publication.

Accepted Manuscripts are published online shortly after acceptance, before technical editing, formatting and proof reading. Using this free service, authors can make their results available to the community, in citable form, before we publish the edited article. We will replace this *Accepted Manuscript* with the edited and formatted *Advance Article* as soon as it is available.

You can find more information about *Accepted Manuscripts* in the Information for Authors.

Please note that technical editing may introduce minor changes to the text and/or graphics, which may alter content. The journal's standard Terms & Conditions and the Ethical guidelines still apply. In no event shall the Royal Society of Chemistry be held responsible for any errors or omissions in this *Accepted Manuscript* or any consequences arising from the use of any information it contains.

ROYAL SOCIETY OF CHEMISTRY

www.rsc.org/materialsA

New hybrid nanocatalyst based on Cu-doped Pd-Fe_3O_4 for tandem synthesis of 2-phenylbenzofurans

Hyunje Woo,[a] Daeho Kim,[a] Ji Chan Park,[b] Ji-Woong Kim,[c] Sungkyun Park,[c] Jae Myung Lee[d] and Kang Hyun Park[a]*

[a] Department of Chemistry and Chemistry Institute for Functional Materials, Pusan National University, Busan 609-735, Korea.
Phone: (+82)-51-510-2238; Fax: (+82)-51-980-5200; e-mail: chemistry@pusan.ac.kr
[b] Clean Fuel Laboratory, Korea Institute of Energy Research, Daejeon, 305-343, Korea.
[c] Department of physics, Pusan National University, Busan 609-735, Korea.
[d] Department of Naval Architecture & Ocean Engineering, Pusan National University, Busan 609-735, Korea.

Abstract

We report a one-pot synthesis of hybrid nanocomposites of Cu-doped Pd-Fe_3O_4 via controlled thermal decomposition of $Fe(CO)_5$ and reduction of $Pd(OAc)_2$ and $Cu(acac)_2$. Sodium oleate, used as a capping agent, affected both the morphologies and surface areas of the Cu-doped Pd-Fe_3O_4 nanocomposites. To the best of our knowledge, these magnetically recyclable hybrid nanocomposites are a new class of nanocatalyst, and the tandem synthesis of 2-phenylbenzofuran from 2-iodophenol with phenylpropiolic acid catalyzed by heterogeneous nanocatalysts has not been reported in the literature. Moreover, Cu-doped Pd-Fe_3O_4 nanocatalyst is superior to previously reported catalysts for this tandem reaction.

Key words

Hybrid; Nanoparticles; Heterogeneous; Catalyst; Tandem reaction

Introduction

In recent years, much effort has been devoted to the synthesis of hybrid multimetallic nanoparticles (NPs), because of their advantages such as high selectivity, catalytic activity, and chemical/physical stability compared with those of the corresponding monometallic components.[1,2] Pd and Fe_3O_4 nanocomposites have attracted much attention because of the high catalytic activity (Pd) and magnetic reusability (Fe_3O_4) of each component in the nanocatalyst. Hybrid Pd-Fe_3O_4 nanocomposites synthesized using various capping agents were previously reported by our group.[3,4] Chen and coworkers[5] reported the synthesis of Pd/Fe_3O_4 heterodimers with controllable interfaces for CO oxidation. Sun et al.[6] reported a one-pot synthesis of sea-urchin-like FePd-Fe_3O_4 nanocomposites, consisting of spherical clusters of FePd NPs with Fe_3O_4 nanorod spikes. These hybrid nanostructures were prepared using various hydrophilic (e.g., trisodium citrate) or hydrophobic (e.g., oleylamine and oleic

Journal of Materials Chemistry A Accepted Manuscript

acid) capping agents.

Until now, the binding selectivity of the capping agents on different crystal facets has affected the anisotropic growth of NPs into various shapes such as cubes, rods, and wires;[7–9] therefore, the use of specific capping agents provides an effective strategy for the synthesis of noble-metal nanocrystals.[10] Catalytic selectivity is also sensitive to the packing of atoms on the surface or the exposed facets of a nanocrystal,[11] and it is, therefore, crucial to identify the interactions between capping agents and NP surfaces clearly to achieve a comprehensive understanding of NP surface chemistry and to optimize the NP properties and performances for various applications.

The privileged 2-substituted benzofuran motif occurs widely in numerous natural products and pharmaceutical compounds.[12] The tandem synthesis of benzofurans from 2-halophenols and terminal alkynes by cross-coupling and subsequent intramolecular hydroalkoxylation is a useful and reliable method.[13] However, this tandem reaction using alkynylcarboxylic acids as coupling partners has not been extensively developed, although alkynylcarboxylic acids are promising alternatives to terminal alkynes because of their high reactivity, simplicity, and ready availability from inexpensive aldehydes.[14,15] Also, carboxylate groups are the leaving groups in cross-coupling, and therefore carbon dioxide is the only byproduct. To the best of our knowledge, the tandem synthesis of 2-phenylbenzofuran from 2-iodophenol with phenylpropiolic acid catalyzed by heterogeneous nanocatalysts has been not reported in the literature. In this work, we developed a facile one-pot synthesis of hybrid nanocomposites of Cu-doped Pd-Fe_3O_4, with a controlled amount of sodium oleate (NaOL; Scheme 1). These hybrid Cu-doped Pd-Fe_3O_4 nanocomposites showed high catalytic activities and stabilities in the tandem synthesis of 2-phenylbenzofurans.

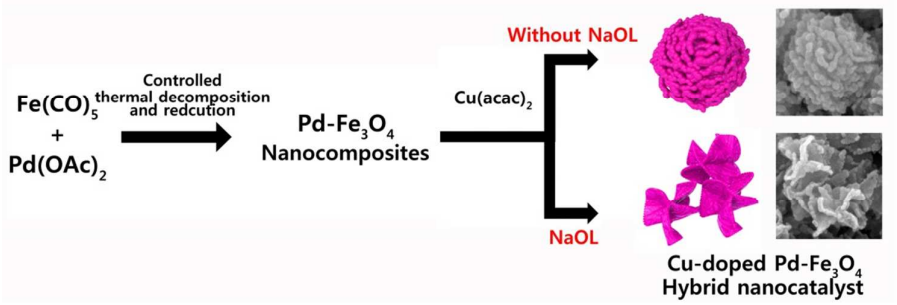

Scheme 1 Synthetic scheme of Cu-doped Pd-Fe_3O_4 nanocomposites.

Experimental

Synthesis of Cu-doped Pd-Fe_3O_4 and Pd-Fe_3O_4-0.3 nanocomposites

A mixture solution of sodium oleate (0.3g) and 1-octadecene (ODE) (10 mL) in a three-necked flask was heated to 200 ℃ under argon flow and magnetic stirring to make sodium oleate dissolved thoroughly. Then the solution was cooled down to room temperature and a

Journal of Materials Chemistry A Accepted Manuscript

mixture of $Pd(OAc)_2$ (0.112 g) and oleylamine (OAm) (10 mL) was added into the solution. The flask was heated to 60 ^oC and further heated to 120 ^oC at a heating rate of 6 ^oC/min. This mixture was kept at this temperature for 30 min. Under a blanket of argon gas, $Fe(CO)_5$ (0.15 ml) was added. Then the solution was further heated to 160 ^oC at a heating rate of 4 ^oC/min and kept at this temperature for 30 min. $Cu(acac)_2$/OAm solution (32 mg/5 ml) was added dropwise in a mixture and heated to 240 ^oC at a heating rate of 2.7 ^oC/min. Then the solution was kept at this temperature for 30 min. The heating source was removed, and the solution was cooled to room temperature. A black product was precipitated by adding ethanol and hexane, and separated by centrifugation.

Pd-Fe_3O_4-0.3 nanocomposites were also synthesized similarly. After $Fe(CO)_5$ was injected, the solution was further heated to 160 ^oC at a heating rate of 4 ^oC/min and kept at this temperature for 30 min. Then, the mixture was further heated to 240 ^oC at a heating rate of 2.7 ^oC/min without addition of $Cu(acac)_2$/OAm solution. The solution was kept at this temperature for 30 min. The heating source was removed, and the solution was cooled to room temperature. A black product was precipitated by adding ethanol and hexane, and separated by centrifugation. The Pd-Fe_3O_4-0.3 nanocomposites were used as a control.

General procedure for tandem synthesis of 2-phenylbenzofurans

The Cu-doped Pd-Fe_3O_4 (generally Cu base: 1 mol% and Pd base: 5.5 mol%), 2-iodophenol (0.056 ml, 0.5 mmol, 1.0 equiv), phenylpropiolic acid (0.088 g, 0.6 mmol, 1.2 equiv), Sodium acetate (0.164 g, 1.0 mmol, 2.0 equiv) and DMSO (5.0 mL) were mixed into a stainless steel reactor. The mixture was vigorously stirred at 130 °C. After the reaction, catalyst was filtered and the reaction mixture was extracted with ethylacetate and water. Drying with $MgSO_4$, filtration, and solvent evaporation of the filtrate yielded the reaction products.

Recyclability tests

After the reaction, the catalyst was separated from the clean solution by centrifugation and decanted by using external magnet. The recovered particles were reused as a catalyst for the next reaction.

Characterization

The morphology of each sample was characterized by transmission electron microscopy (TEM) (Omega EM912 operated at 120 kV, Korea Basic Science Institute, and a Tecnai G2 F30 operated at 300 kV, KAIST) by placing a few drops of the corresponding colloidal solution on carbon-coated copper grids (200 mesh, F/C coated, Ted Pella Inc., Redding, CA, USA). FE-scanning electron microscopy (SEM) (HITACHI_ S_4800, National Nanofab Center, South Korea) was also used for analyses. Magnetization data were taken using a superconducting quantum interference device (SQUID) (MPMS-7, Quantum design). The X-ray powder diffraction (XRD) patterns were recorded on a Rigaku D/MAX-RB (12 kW) diffractometer. X-ray photoelectron spectroscopy (XPS) (Theta Probe, Thermo) was

Journal of Materials Chemistry A Accepted Manuscript

employed to measure the structural and chemical properties of the nanocomposites. The tandem reaction products were analyzed by ^{1}H nuclear magnetic resonance (NMR) spectroscopy using a Varian Mercury Plus (300 MHz). Chemical shift values were recorded as parts per million (ppm) relative to tetramethylsilane as an internal standard unless otherwise indicated, and coupling constants are given in Hz. Mass spectra were obtained on Shimadzu GC/MS QP-2010 SE (EI) (Pusan National University).

Results

Characterization of the hybrid Cu-doped Pd-Fe_3O_4 catalyst

The Cu-doped Pd-Fe_3O_4 nanocomposites were synthesized by facile decomposition of $Fe(CO)_5$ and reduction of $Pd(OAc)_2$ and $Cu(acac)_2$ in OAm and ODE. In the synthesis, $Pd(OAc)_2$ (0.114 g), OAm (10 mL), ODE (10 mL), and a controlled amount of NaOL were mixed at 60 °C and then heated to 120 °C at a heating rate of 6 °C/min. The mixture was kept at this temperature for 30 min. $Fe(CO)_5$ (0.15 mL) was added under argon gas, and the solution was heated to 160 °C at a heating rate of 4 °C/min and kept at 160 °C for 30 min. $Cu(acac)_2$ (32 mg) in OAm was added; the mixture was heated to 240 °C and kept at this temperature for 30 min. The mixture was cooled to room temperature. The sample was centrifuged in ethanol and hexane, giving a black precipitate. The products were analyzed using inductively coupled plasma-atomic emission spectroscopy (ICP-AES). The Pd/Fe/Cu molar ratios in the Cu-doped Pd-Fe_3O_4 nanocomposites synthesized at 240 °C were controlled at 30:63:7 to 36:55:9 by increasing the amount of NaOL from 0 to 0.5 g (Table 1).

Table 1. ICP molar ratio and BET surface area of hybrid nanocomposites.

	Pd	Fe	Cu	BET surface area (m^2/g)
Pd-Fe_3O_4-0.3	42	58	-	7.30
Cu-doped Pd-Fe_3O_4-0	30	63	7	28.2
Cu-doped Pd-Fe_3O_4-0.3	36	54	10	31.2
Cu-doped Pd-Fe_3O_4-0.5	36	55	9	34.1

Journal of Materials Chemistry A Accepted Manuscript

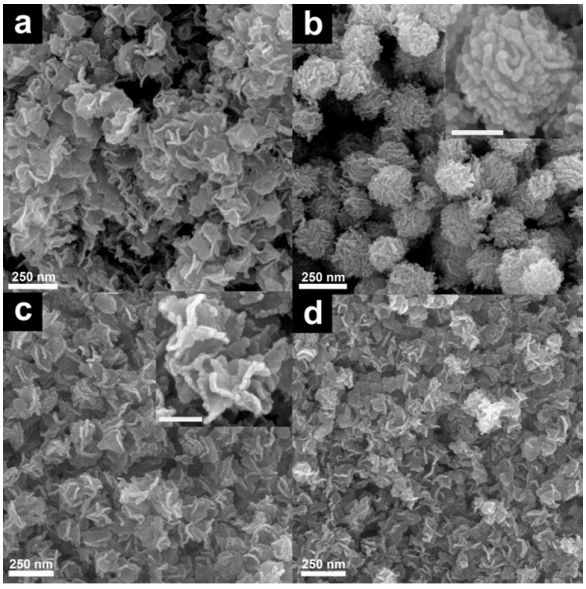

Fig. 1 SEM images of (a) Pd-Fe_3O_4, (b) Cu-doped Pd-Fe_3O_4-0, (c) Cu-doped Pd-Fe_3O_4-0.3 and (d) Cu-doped Pd-Fe_3O_4-0.5 hybrid nanocomposites. The bars in the inset represent (b,c) 100 nm.

Fig. 1 shows scanning electron microscopy images of the Pd-Fe_3O_4-0.3 and Cu-doped Pd-Fe_3O_4-*n* hybrid nanocomposites, synthesized using different amounts of NaOL; *n* denotes the amount of NaOL (g) in the reaction mixture. As a control experiment, a Pd-Fe_3O_4-0.3 nanocomposite was synthesized without addition of the $Cu(acac)_2$ precursor (Fig. 1a). In the absence of NaOL (Cu-doped Pd-Fe_3O_4-0), spherical structures, with an average diameter of 215 nm, were obtained (Fig. 1b).

Interestingly, when the NaOL capping agent was added, hybrid Cu-doped Pd-Fe_3O_4 nanocomposites showed sheet-assembled structure not spherical shape (Fig. 1c and d). Transmission electron microscopy (TEM) images of the Pd-Fe_3O_4-0.3 and Cu-doped Pd-Fe_3O_4-*n* nanocomposites are also shown in Fig. 2. The Pd-Fe_3O_4-0.3 nanocomposites did not grow well, and consisted of seed-like nanostructures (Fig. 2a). When the amount of NaOL was increased (0.5 g), the morphology was slightly decomposed (Fig. 2c and d). Low-resolution TEM images of the Cu-doped Pd-Fe_3O_4-*n* nanocomposites are shown in Fig. S1.

Journal of Materials Chemistry A Accepted Manuscript

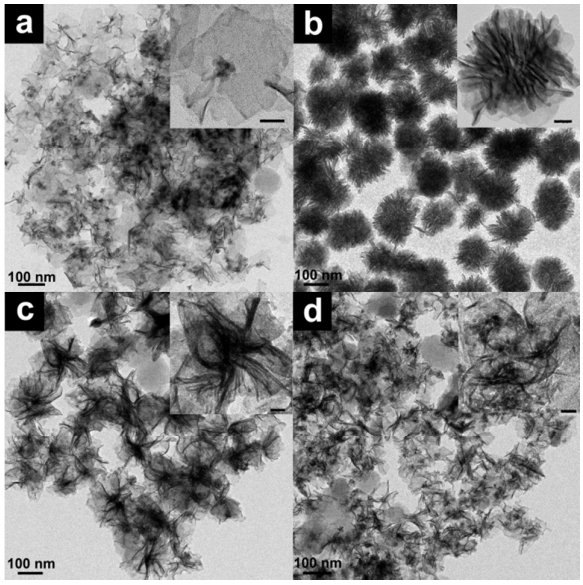

Fig. 2 TEM images of (a) Pd-Fe_3O_4, (b) Cu-doped Pd-Fe_3O_4-0, (c) Cu-doped Pd-Fe_3O_4-0.3 and (d) Cu-doped Pd-Fe_3O_4-0.5 hybrid nanocomposites. The bars in the inset represent 20 nm.

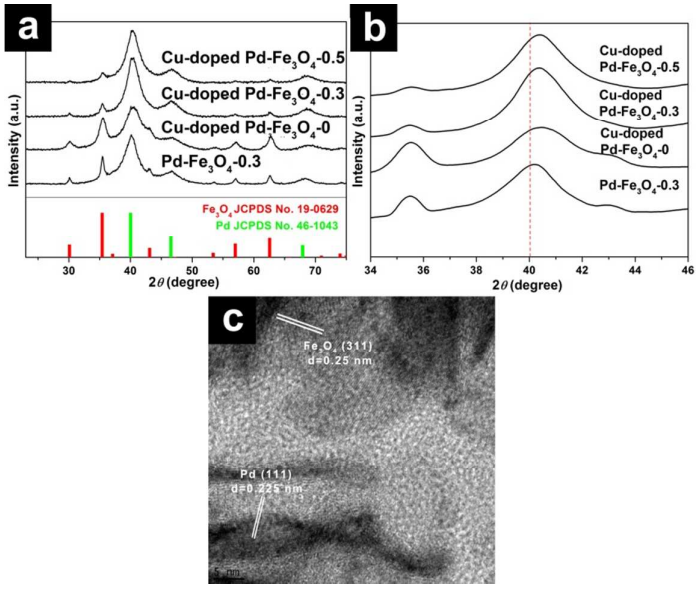

Fig. 3 (a,b) XRD patterns of Pd-Fe_3O_4 and Cu-doped Pd-Fe_3O_4 and (c) HR-TEM image of Cu-doped Pd-Fe_3O_4 -0.3.

The crystal structures of the Cu-doped Pd-Fe_3O_4-*n* nanocomposites were determined using X-ray diffraction (XRD; Fig. 3a). All the peaks in the XRD patterns can be assigned to the (111), (200), and (220) lattice planes of a face-centered cubic (fcc) Pd crystal structure, and the (220), (311), (422), (511), and (440) lattice planes of the cubic spinel structure of Fe_3O_4 (JCPDS No. 19-0629). The magnified image in Fig. 3b shows that the diffraction peak of Cu-doped Pd at around 40° shifted to a higher angle than that of Pd. This shifts indicates Pd

Journal of Materials Chemistry A Accepted Manuscript

lattice contraction caused by replacing fcc Pd atoms with Cu.[16,17] A high-resolution TEM image of the Cu-doped Pd-Fe_3O_4-0.3 nanocomposite (Fig. 3c) shows that the Pd and Fe_3O_4 have well-defined structures and uniformly spaced lattice fringes, with fringe distances of 0.225 nm for the Pd (111) plane and 0.25 nm for the Fe_3O_4 (311) plane, corresponding to fcc Pd and Fe_3O_4 structures, respectively. The high-angle annular dark-field scanning TEM image and elemental mappings of Cu, Pd, and Fe also show that Cu-doped Pd and Fe_3O_4 are dispersed in all areas of the composite, confirming the hybrid Cu-doped Pd-Fe_3O_4 structure (Fig. 4).

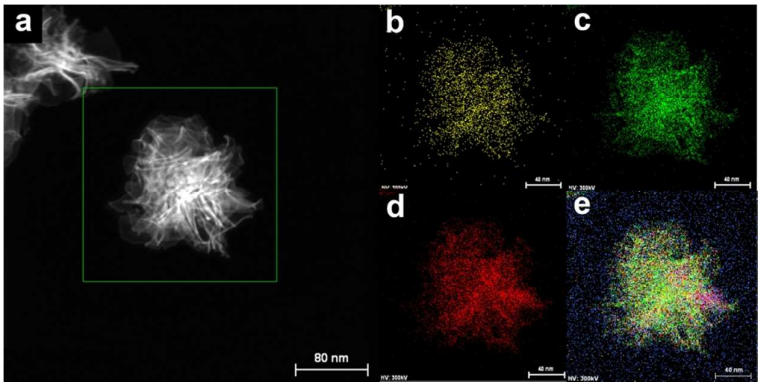

Fig. 4 (a) HAADF-STEM image of Cu-doped Pd-Fe_3O_4-0.3 and elemental mapping of (b) Cu, (c) Pd, (d) Fe and (e) overlap.

Sheet-assembled structures are widely used for sensors, lithium-ion batteries, and photocatalysts, because of their large specific surface areas.[18] The Brunauer–Emmett–Teller (BET) surface areas of Pd-Fe_3O_4-0.3, and Cu-doped Pd-Fe_3O_4-0, -0.3, and -0.5 nanocomposites were calculated to be 7.30, 28.2, 31.2, and 34.1 m^2g^{-1}, respectively (Table 1). These values are much higher than those for previously reported hollow and solid Fe_3O_4 microspheres (12.27 and 5.43 m^2g^{-1}), because of the individual nanosheet structures.[19] A high amount of NaOL increased the BET surface areas of the Cu-doped Pd-Fe_3O_4 nanocomposites, demonstrating the effect of NaOL on the surface area and morphology. However, it is unclear how NaOL capping agents affect the nanocomposite morphology during the growth step. To clarify the synthetic mechanism, the reaction mixture was immediately transferred to an ice-bath to quench the synthesis when the temperature reached 160 °C. We assume that Pd-Fe_3O_4 seed particles are first formed and then self-aggregate before the nanosheets start to grow on the surfaces of the Pd-Fe_3O_4 seed aggregates (Fig. 5). Fig. S2 shows TEM images of Cu-doped Pd-Fe_3O_4-0.3 nanocomposites synthesized at different temperatures (160 and 200 °C). Although the nanocomposite seeds were well synthesized, the temperatures were not high enough for thermal decomposition of $Fe(CO)_5$ and reduction of $Pd(OAc)_2$ and $Cu(acac)_2$, resulting in poor growth, and Pd-Fe_3O_4-0.3 seeds remained in the nanocomposites.

Journal of Materials Chemistry A Accepted Manuscript

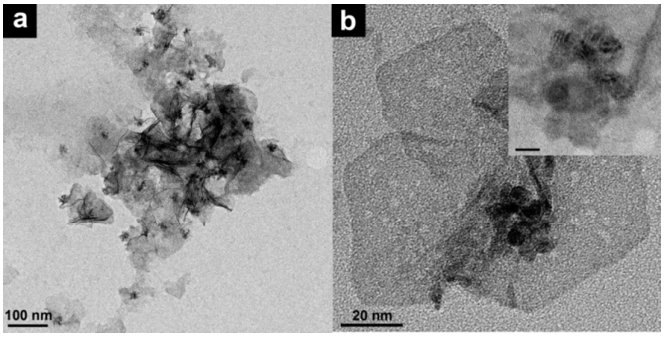

Fig. 5 Pd-Fe_3O_4-0.3 seed aggregates (Reaction mixture was immediately transferred into ice-bath to quench further synthesis when the temperature was reached to 160 °C.). The bars in the inset represent 5 nm.

Elemental analysis of Cu-doped Pd-Fe_3O_4-0.3 was performed using X-ray photoelectron spectroscopy (XPS; Fig. 6). The wide-scan XPS spectra of Cu-doped Pd-Fe_3O_4-0.3 shows photoelectron lines at a binding energy of about 285.5 eV, attributed to C 1s (Fig. 6a). There are two Cu $2p_{3/2}$ peaks, for Pd–Cu and Cu_2O, which can be clearly distinguished from those of Cu. The binding energy of the Pd–Cu peak (931.8 eV) is lower than that that of Cu metal (932.3 eV); these Cu peak shifts are indicative of the formation of Pd-Cu bimetallic particles (Fig. 6b).[20] The Cu $2p_{3/2}$ peak for Cu_2O (932.9 eV) is shifted slightly to higher binding energy, by 0.6 eV, compared with that of Cu.[21] In the Fe 2p spectrum (Fig. 6c), the Fe $2p_{1/2}$ and Fe $2p_{3/2}$ peaks are located at 710.8 and 724.3 eV, not at 709.9 and 723.5 eV as in the case of γ-Fe_2O_3.[22] For Pd, the most intense peaks are observed at binding energies of around 335.1 ($3d_{5/2}$) and 340.3 ($3d_{3/2}$) eV, respectively, indicating metallic Pd characteristics (Fig. 6d). The superconducting quantum interference device data show the magnetic curves as a function of the applied field at 300 K (Fig. S3). The saturation magnetization value of the Cu-doped Pd-Fe_3O_4-0.3 nanocomposite was 9.2 emu·g^{-1}. Moreover, both the remanence and coercivity of the nanocomposite were close to zero, indicating superparamagnetism.

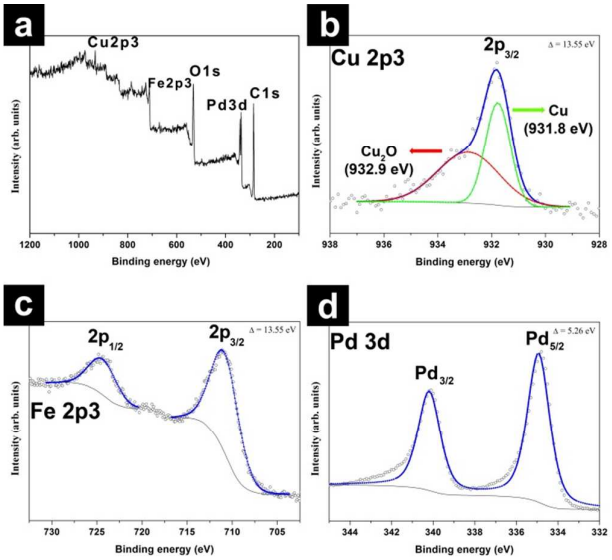

Journal of Materials Chemistry A Accepted Manuscript

Fig. 6 The XPS spectra of Cu-doped Pd-Fe_3O_4-0.3 nanocomposites.

Table 2 Tandem synthesis of 2-phenybenzofurans.

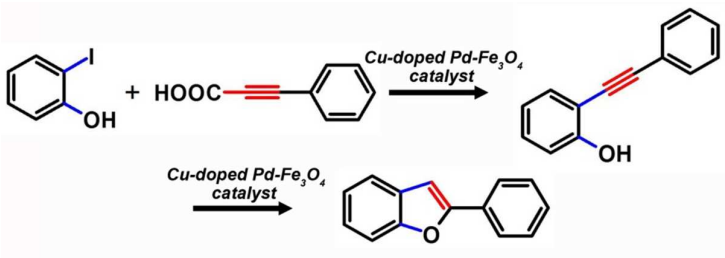

Entry	Catalyst	Time (h)	Base	Conv. (%)[a]
1	Cu-doped Pd-Fe_3O_4-0	1	NaOAc	36[b]
2	Cu-doped Pd-Fe_3O_4-0	1	NaOAc	52[c]
3	Cu-doped Pd-Fe_3O_4-0	1	NaOAc	90
4	Cu-doped Pd-Fe_3O_4-0	1	LiOAc	54
5	Cu-doped Pd-Fe_3O_4-0	1	Cs_2CO_3	45
6	Cu-doped Pd-Fe_3O_4-0.3	1	NaOAc	95
7	Cu-doped Pd-Fe_3O_4-0.5	1	NaOAc	54
8	Pd-Fe_3O_4-0.3	1	NaOAc	7
9	Cu-doped Pd-Fe_3O_4-0.3	1	NaOAc	15[d]
10	Cu-doped Pd-Fe_3O_4-0.3	0.5	NaOAc	83
11	Cu-doped Pd-Fe_3O_4-0.3	1	NaOAc	46[e]

Reaction condition: Cu-doped Pd-Fe_3O_4 catalyst (Cu base: 1.0 mol%, Pd base: 5.5 mol%), 2-iodophenol (0.5 mmol), phenylpropiolic acid (0.6 mmol), base (1.0 mmol), solvent (5.0 ml) Reaction temperature: 130 °C. [a] Determined by using GC-MS spectroscopy based on 2-iodophenol. [b,c] DMF and NMP were used as solvent, respectively. [d] Reaction was conducted at 100 °C. [e] 0.5 mol% of catalyst (Cu base) was used.

Tandem synthesis of 2-phenybenzofurans

The catalytic activity of Cu-doped Pd-Fe_3O_4 was investigated, using the tandem synthesis of 2-phenylbenzofurans from 2-iodophenols with phenylpropiolic acids as a model reaction, under various conditions (Table 2). First, the effect of the solvent was examined in the presence of Cu-doped Pd-Fe_3O_4-0 at 130 °C for 1 h (Table 2, entries 1-3). The use of a more polar solvent (DMSO) led to an increase in the conversion, because of the superior solubility of the reactant and catalyst in the reaction medium. The influences of bases such as NaOAc, LiOAc, and Cs_2CO_3 in the standard reaction were also studied (Table 2, entries 3-5). Better conversion was achieved with NaOAc (90%) than with LiOAc and Cs_2CO_3. Among the Cu-

Journal of Materials Chemistry A Accepted Manuscript

doped Pd-Fe_3O_4-*n* catalysts, Cu-doped Pd-Fe_3O_4-0.3 showed the highest catalytic activity (Table 2, entries 3, 6, and 7). Although the Cu-doped Pd-Fe_3O_4-0.5 nanocomposites had the highest surface area, a low conversion was obtained because of destruction of the catalyst structure. Pd-Fe_3O_4-0.3 was used in a control experiment, and the catalytic activity was significantly lower without copper (Table 2, entry 8). Until now, multimetallic catalytic tandem reactions have attracted much attention because they avoid the need for tedious intermediate separation processes; this significantly lowers energy consumption and the cost of the final products.[23] Bimetallic catalytic systems also have higher catalytic activities than single-metal catalytic systems, because of electron transfer across the metal-metal interface. The catalytic activity of Cu-doped Pd-Fe_3O_4-*n* was therefore better than that of Pd-Fe_3O_4-0.3 because of the presence of copper, which is efficient in activating phenylpropiolic acid, and the low surface area of Pd-Fe_3O_4-0.3 (7.30 m^2g^{-1}; Table 2, entries 5 and 6).[24] As expected, 15 % conversion was achieved at low temperature (100 °C; Table 2, entries 6 and 9). We also tested the effects of the amount of catalyst and reaction time. The conversions were lower (83% and 46%) when a short reaction time (0.5 h) and a smaller amount of catalyst (Cu base: 0.5 mol), respectively, were used (Table 2, entries 10 and 11). The optimum reaction conditions were found to be as follows: Cu-doped Pd-Fe_3O_4-0.3 (Cu base: 1.0 mol%, Pd base: 5.5 mol%); solvent: DMSO (5.0 mL); temperature: 130 °C; and reaction time: 1 h (Table 2, entry 6). The catalytic activity of Cu-doped Pd-Fe_3O_4-0.3, without any additives and ligands, was better than those previously reported for a homogeneous CuI catalyst, in terms of the turnover frequency (TOF).[14] We also compared the catalytic activity with those heterogeneous catalysts previously reported by our group (Fig. 7).[3,4,25,26] Among them, Cu-doped Pd-Fe_3O_4-0.3 showed the highest TOF under given conditions; this can be attributed to the dual-catalytic effect of Pd and Cu. After the tandem reaction, the Cu-doped Pd-Fe_3O_4-0.3 catalyst could be totally separated using an external magnet, because of the superparamagnetic properties of Fe_3O_4 particles.[27] The Cu-doped Pd-Fe_3O_4-0.3 catalyst was recycled ten times and its initial high activity (>91%) was maintained, without any loss, during recycling (Fig. S4). The morphology and crystal structure of the Cu-doped Pd-Fe_3O_4 nanocomposites remained almost unchanged after the reaction (Fig. S5). In Pd and Cu leaching tests, the filtered solution after the catalytic reaction was checked using ICP-AES; small amounts of Pd and Cu, 1.62 and 9.00 ppm, respectively, were detected in the solution. We can conclude that in the Cu-doped Pd-Fe_3O_4-0.3 nanocomposite, the Cu-doped Pd has high catalytic activity, and high stability was confirmed through recycling and leaching tests.

Journal of Materials Chemistry A Accepted Manuscript

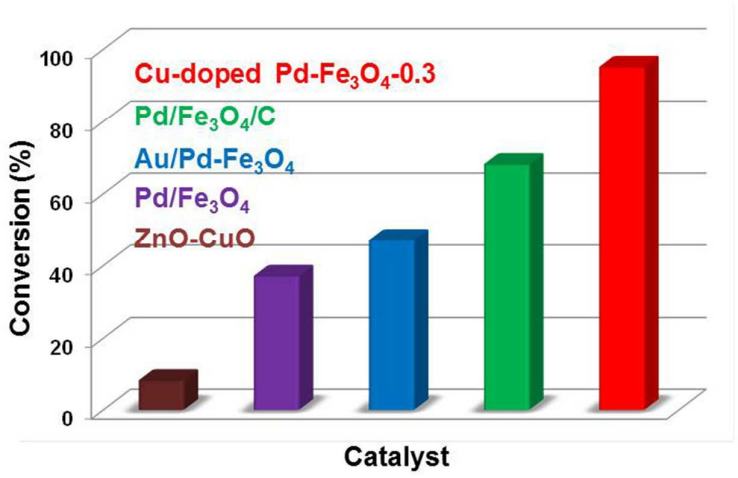

Fig. 7 Comparison of catalytic activity with previous reported heterogeneous catalysts in our group. Reaction condition: 2-iodophenol (0.5 mmol), phenylpropiolic acid (0.6 mmol), NaOAc (1.0 mmol), DMSO (5.0 ml), Catalyst (1.0 mol%), 130 °C, 1 h.

In conclusion, we successfully developed a one-pot synthesis of Cu-doped Pd-Fe_3O_4 hybrid nanocomposites through controlled thermal decomposition of $Fe(CO)_5$ and reduction of $Pd(OAc)_2$ and $Cu(acac)_2$. NaOL affected both the morphology and surface area of the hybrid of the Cu-doped Pd-Fe_3O_4. The synthesized Cu-doped Pd-Fe_3O_4-0.3 hybrid catalyst showed high catalytic activity in the tandem synthesis of 2-phenylbenzofurans and was magnetically recyclable. The same concept could be extended to other multimetallic NP systems, making it possible to tune NP catalysis for many different chemical reactions.

Acknowledgment

This research was supported by Basic Science Research Pro-gram through the National Research Foundation of Korea (NRF) funded by the Ministry of Science, ICT & Future Plan-ning (No.2013R1A1A1A05006634) and GCRC-SOP (No.2011-0030013). K. H. P thanks to the TJ Park Junior Faculty Fellowship and LG Yonam Foundation. S. P thanks for the support by KAERI and KBSI (E35800).

References

Journal of Materials Chemistry A Accepted Manuscript

1 Q. Tan, C. Du, Y. Sun, G. Yin and Y. Gao, *J. Mater. Chem. A*, 2014, **2,** 1429-1435.

2 L. Tan, X. Wu, D. Chen, H. Liu, X. Meng and F. Tang, *J. Mater. Chem. A*, 2013, **1,** 10382-10388.

3 H. Woo, K. Lee and K. H. Park, *ChemCatChem*, 2014, **6**, 1635-1640.

4 H. Woo, J. C. Park, S. Park and K. H. Park, *Nanoscale*, 2015, **7**, 8356-8360.

5 S. Chen, R. Si, E. Taylor, J. Janzen and J. Chen, *J. Phys. Chem. C*, 2012, **116**, 12969-12976.

6 Y. Yu, K. Sun, Y. Tian, X.-Z. Li, M. J. Kramer, D. J. Sellmyer, J. E. Shield and S. Sun, *Nano Lett.*, 2013, **13**, 4975-4979.

7 C. Wang, H. Daimon, Y. Lee, J. Kim and S. Sun, *J. Am. Chem. Soc.*, 2007, **129**, 6974-6975.

8 Y. Yin and A. P. Alivisatos, *Nature*, 2005, **437**, 664-670.

9 C. Wang, Y. J. Hu, C. M. Lieber and S. Sun, *J. Am. Chem. Soc.*, 2008, **130**, 8902-8903.

10 S. Xie, H. Zhang, N. Lu, M. Jin, J. Wang, M. J. Kim, Z. Xie and Y. Xia, *Nano Lett.*, 2013, **13**, 6262-6268.

11 Y. Xia, Y. Xiong, B. Lim and S. E. Skrabalak, *Angew. Chem. Int. Ed.*, 2009, **48**, 60-103.

12 J. Zhang, L. Li, Y. Wang, W. Wang, J. Xue and Y. Li, *Org. Lett.*, 2012, **14**, 4528-4530.

13 R. P. Wang, S. Mo, Y. Z. Lu and Z. M. Shen, *Adv. Synth. Catal.*, 2011, **353**, 713-718.

14 D. Zhao, C. Gao, X. Su, Y. He, J. You and Y. Xue, *Chem. Commun.*, 2010, **46**, 9049-9051.

15 J. P. Das, U. K. Roy and S. Roy, *Organometallics*, 2005, **24**, 6136-6140.

16 S. Diyarbakir, H. Can and Ö. Metin, *ACS Appl. Mater. Interfaces*, 2015, **7**, 3199-3206.

17 K. Mandal, D. Bhattacharjee, P. S. Roy, S. K. Bhattacharya and S. Dasgupta, *Applied Catalysis A: General*, 2015, **492**, 100-106.

18 X. Liu, J. Zhang, L. Wang, T. Yang, X. Guo, S. Wu and S. Wang, *J. Mater. Chem.*, 2011, **21**, 349-356.

19 Q. Q. Xiong, J. P. Tu, Y. Lu, J. Chen, Y. X. Yu, Y. Q. Qiao, X. L. Wang and C. D. Gu, *J. Phys. Chem.*, C 2012, **116**, 6495-6502.

20 B. L. Gustafson and P. S. Wehner, *Appl. Surf. Sci.*, 1991, **52**, 261-270.

21 D. Tahir and S. Tougaard, *J. Phys.: Condens. Matter*, 2012, **24**, 175002.

Journal of Materials Chemistry A Accepted Manuscript

22 V. Chandra, J. Park, Y. Chun, J. W. Lee, I.-C. Hwang and K. S. Kim, *ACS Nano*, 2010, **4**, 3979-3686.

23 M. J. Climent, A. Corma, S. Iborra and M. J. Sabater, *ACS Catal.*, 2014, **4**, 870-891.

24 X. Qu, T. Li, P. Sun, Y. Zhu, H. Yang and J. Mao, *Org. Biomol. Chem.*, 2011, **9**, 6938-6942.

25 H. Woo, K. Lee, J. C. Park and K. H. Park, *New J. Chem.*, 2014, **38**, 5626-5632.

26 J. C. Park, A Y. Kim, J. Y. Kim, S. Park, K. H. Park and H. Song, *Chem. Commun.*, 2012, **48**, 8484-8486.

27 H. Zhang, G. Zhang, X. Bi and X. Chen, *J. Mater. Chem. A*, 2013, **1,** 5934–5942.

Journal of Materials Chemistry A Accepted Manuscript

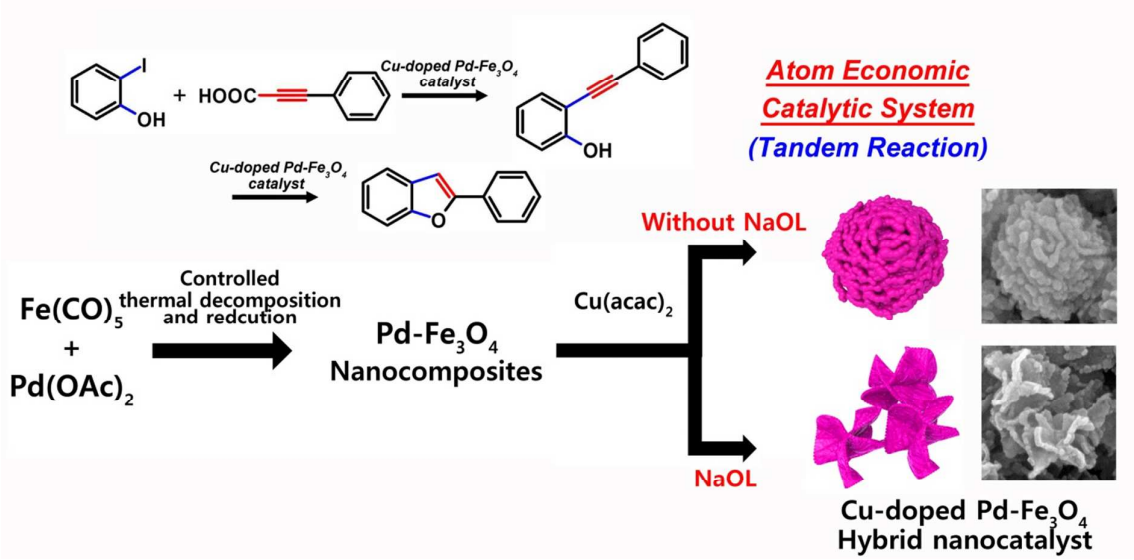

Journal of Materials Chemistry A Accepted Manuscript